Vision Research 177 (2020) 20–31

Contents lists available at ScienceDirect

Vision Research

journal homepage: www.elsevier.com/locate/visres

A decision-time account of individual variability in context-dependent orientation estimation

Ron Dekel, Dov Sagi*

Department of Neurobiology, The Weizmann Institute of Science, Rehovot 7610001, Israel

ARTICLE INFO

Keywords:
Visual adaptation
Tilt aftereffect
Tilt illusion
Reaction time
Drift diffusion model
Orientation bias
Individual differences

ABSTRACT

Following exposure to an oriented stimulus, the perceived orientation is slightly shifted, a phenomenon termed the tilt aftereffect (TAE). This estimation bias, as well as other context-dependent biases, is speculated to reflect statistical mechanisms of inference that optimize visual processing. Importantly, although measured biases are extremely robust in the population, the magnitude of individual bias can be extremely variable. For example, measuring different individuals may result in TAE magnitudes that differ by a factor of 5. Such findings appear to challenge the accounts of bias in terms of learned statistics: is inference so different across individuals? Here, we found that a strong correlation exists between reaction time and TAE, with slower individuals having much less TAE. In the tilt illusion, the spatial analogue of the TAE, we found a similar, though weaker, correlation. These findings can be explained by a theory predicting that bias, caused by a change in the initial conditions of evidence accumulation (e.g., priors), decreases with decision time (*Communications Biology 3 (2020) 1–12). We contend that the context-dependence of visual processing is more homogeneous in the population than was previously thought, with the measured variability of perceptual bias explained, at least in part, by the flexibility of decision-making. Homogeneity in processing might reflect the similarity of the learned statistics.

1. Introduction

Visual context, from space and time, is known to influence the processing of visual information. Using basic visual properties, such as orientation, motion, and color, clear behavioral and electrophysiological effects have been identified (Clifford & Rhodes, 2005; Clifford et al., 2007; Gibson & Radner, 1937; Gibson, 1937; Kohn, 2007; Lamme & Roelfsema, 2000; Webster, 2011, 2015). With orientation features, the contextual orientation is known to lead to a perceptually salient shift in the perceived orientation (Gibson & Radner, 1937; Gibson, 1937; Schwartz, Hsu, & Dayan, 2007). When the context surrounds a target, this phenomenon is referred to as the tilt illusion (TI, Fig. 1A, Clifford, 2014; Gibson, 1937), and when the context precedes a target in time, it is referred to as the tilt aftereffect (TAE, Fig. 1B, Gibson & Radner, 1937; Webster, 2015). In both space and time (Schwartz et al., 2007), a contextual orientation of 20° clockwise to vertical leads to a *counterclockwise* shift in the estimated orientation, by a few degrees (see Fig. 1).

Extensive theoretical work has been done to better understand such context effects. Generally, context-dependent changes in visual processing are thought to be functionally useful, despite some debate regarding details (Kohn, 2007; Schwartz, Snow, & Coen-Cagli, 2017; Solomon & Kohn, 2014; Clifford, 2014; Webster, 2011). Possible benefits include (a) self-calibration, constancy, or correction of a reference "norm" (Andrews, 1964; Day, 1972; Dekel & Sagi, 2020a; Gibson & Radner, 1937; Webster, 2011), (b) optimization of the neural code, such as improved gain of computational units, improved coding sensitivity to likely events, or decorrelation to remove coding redundancies (Benucci, Saleem, & Carandini, 2013; Coen-Cagli, Kohn, & Schwartz, 2015; Pinchuk-Yacobi & Sagi, 2019; Snow et al., 2017; Wei & Stocker, 2017), and (c) enhanced attentional selection of novel or surprising events (such events are presumably more likely to be important and hence deserve more attention). However, these and other alternatives are not necessarily mutually exclusive (e.g., orientation biases may reflect both self-calibration and decorrelation, Clifford, Wenderoth, and Spehar (2000)), and are not necessarily dependent on the neural implementation (e.g., divisive normalization may underlie both code optimization and attentional selection, Carandini & Heeger, 2012). However, two general observations can be made: First, theories seem to differ based on the speculated purpose (Press, Kok, & Yon, 2020), making perception more veridical (e.g., self-calibration), or less veridical but better at a given task (e.g., code optimization). Second, theories differ in how the effect is thought to depend on the computational constraints of the system. That is, if the system were to have better

* Corresponding author.
E-mail address: Dov.Sagi@Weizmann.ac.il (D. Sagi).

https://doi.org/10.1016/j.visres.2020.08.002
Received 24 November 2019; Received in revised form 16 July 2020; Accepted 10 August 2020

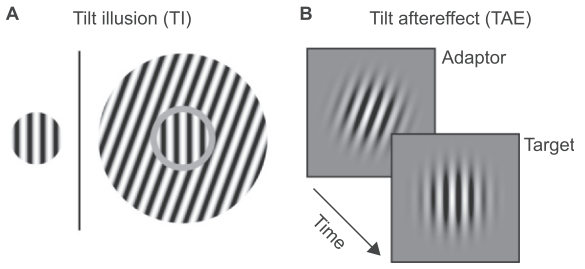

Fig. 1. Tilt illusion and tilt aftereffect. (A) In the tilt illusion (TI), an oriented surround leads to a shift in perceived orientation. Right: the surrounding annulus, oriented 20° clockwise to vertical, leads to a counterclockwise shift in the perceived orientation of the center circle (the target). Left: the target without surround, was provided as a reference for the reader and was not used in the experiments. (B) In the tilt aftereffect (TAE), exposure to an oriented adaptor (e.g., +20°) leads to a shift in the perceived orientation of a subsequently viewed target (in the same direction as in TI).
Figure reproduced from Dekel & Sagi, 2020b

computational abilities (e.g., more neurons, more neural bandwidth), would context-dependent biases be less pronounced? For example, if biases reflect calibration based on the "true" white (white balance) or the "true" vertical, then it seems reasonable to assume that the biases are *not* dependent on computational constraints, and rather, are determined by a system-independent inference process (using stimulation statistics, such as the average color or the orientation modes). Alternatively, if biases reflect a tradeoff between computational constraints (such as limited bandwidth) and perceptual error, then we would expect less bias in a better system.

An interesting source of theory-diagnostic information can be obtained by considering individual differences in vision (Grzeczkowski, Clarke, Francis, Mast, & Herzog, 2017; Mollon, Bosten, Peterzell, & Webster, 2017). In the TI, as well as in other spatial-context-dependent biases, individual measures showed large differences (by an order of magnitude), with strong test–retest reliability (Grzeczkowski et al., 2017; Song, Schwarzkopf, & Rees, 2013). These differences were found to be correlated with variability in orientation JND (just-noticeable-differences, showing an R^2 value of ~60%) and were thought to reflect variability in the size of area V1 across individuals (Schwarzkopf, Song, & Rees, 2011; Song et al., 2013). These results seem consistent with an account of variability in terms of fixed neuronal constraints of low-level vision. In the TAE, direct investigation of individuality has, to the best of our knowledge, never been attempted, despite the large individuality evident in the literature (Gibson & Radner, 1937; Knapen, Rolfs, Wexler, & Cavanagh, 2010; Magnussen & Johnsen, 1986; Wolfe, 1984).

Importantly, we recently reported that context-dependent bias is much stronger in fast compared with slow reaction times (RT) of an individual (Dekel & Sagi, 2020b). This effect was largely independent of orientation sensitivity (i.e., JND). Moreover, we suggested that this within-observer variability in bias is explained by the theory that decision makers integrate evidence over time to reduce error, with an initial state of accumulation that is set by prior evidence favoring one decision outcome over others (Gold & Shadlen, 2007; Ratcliff, 1978; Ratcliff, Smith, Brown, & McKoon, 2016; Salkind, 2012). In such models, bias, caused by the initial conditions, is expected to gradually decrease with decision time owing to noise accumulation, leading to a dramatic reduction of bias in slower decisions (Dekel & Sagi, 2020b; Mulder, Wagenmakers, Ratcliff, Boekel, & Forstmann, 2012; Ratcliff & McKoon, 2008; Summerfield & De Lange, 2014; White and Poldrack, 2014).

Here, we investigated individual differences in both TI and TAE, and considered their previously unexplored interaction with RT. Importantly, we found a strong negative correlation between TAE and RT, and a similar albeit statistically weaker correlation between TI and RT. These findings suggest that individual differences are based on RT, which complements current knowledge of differences in terms of orientation JND. This account is consistent with fixed low- and variable high-level visual processing.

2. Methods

This study re-analyzed experimental data used in Dekel and Sagi (2020b).

2.1. Observers

Twenty-nine observers (23 females, 6 males, age 18–40y) with normal or corrected-to-normal vision participated in the experiments. All observers were naïve to the purpose of the experiments, and provided their written informed consent. Most observers had prior experience of participation in psychophysical experiments, but during the main experiment (TAE periphery), all observers short of one were new to the task and the stimuli. The inclusion/exclusion criteria were the same for all experiments: observers were recruited by advertisement, and were refused participation if they did not pass an eye examination. The number of daily repetitions and experiments per observer was determined by the observers' availability. The work was carried out in accordance with the Code of Ethics of the World Medical Association (Declaration of Helsinki) and was approved by the Institutional Review Board (IRB) of the Weizmann Institute of Science.

2.2. Apparatus

The stimuli were presented on a 22″ HP p1230 monitor operating at 85 Hz with a resolution of 1600 × 1200 that was gamma-corrected (linearized). The mean luminance of the display was 26 cd·m^{-2} (TAE experiments) or 49 cd·m^{-2} (TI experiments) in an otherwise dark environment. The monitor was viewed at a distance of 100 cm.

2.3. Stimuli and tasks

The stimuli were presented using dedicated software. For the TAE experiments, we used the "Psy" program developed by Yoram Bonneh. For the TI experiments, we used a browser-based software described in Dekel and Sagi (2020a), Dekel and Sagi (2020b). Estimations of timing accuracy in both setups suggest single video-frame accuracy in stimulus presentation on almost all trials, and RT measurements within ~10 ms of the true key-presses time.

All stimuli were presented on a uniform gray background. To begin stimulus presentation in a trial, observers fixated on the center of the display and pressed the spacebar (self-initiated trials). Responses were provided using the left and right arrow keys. Observers were informed that they are permitted to reply as fast as they wish, as long as reply speed did not lead to cases where they were certain of the target tilt (clockwise vs. counter-clockwise) but pressed the wrong key (finger errors).

TAE experiments. The following presentation sequence was used (Fig. 1B): a blank screen (600 ms presentation), a Gabor "adaptor" (i.e., context, oriented randomly in each trial −20° or +20° to vertical, 50 ms), a blank screen (600 ms), and a near-vertical Gabor "target" (50 ms). Observers were instructed to inspect the adaptor and target presentations, and then to report whether the orientation of the target was clockwise or counter-clockwise to vertical (no feedback). Gabor patches were 50% Michelson contrast, with a Gaussian envelope of $\sigma = 0.42°$ and a sine wavelength of $\lambda = 0.3°$ having a random phase. Two versions of the experiment were run: "periphery" and "fixation", referring to the retinal position at which both targets and adaptors were presented. In the periphery experiment, adaptors and targets were presented at either left or right of the fixation (at ± 1.8° eccentricity), and the target was randomly presented either at the same side as the adaptor (retinotopic measurement) or at the opposite side (non-

retinotopic measurement). Targets were oriented from −12° to +12° in steps of 2° (a total of 13 possible orientations). In the fixation experiment, adaptors and targets were presented at the fixated center of the display. Targets were oriented −9° to +9° in steps of 1° (a total of 19 possible orientations). In both versions of the experiment, four peripheral crosses co-appeared with the target to improve the discrimination between adaptor and target.

TI experiments. Stimuli (Fig. 1A right) consisted of a sine-wave circular "target" (radius of 0.6°) and a sine-wave annulus "surround" (width of 1.2°, and a gap of 0.15° from the central circle). Targets were oriented from −9° to +9° in steps of 1°, with $\lambda = 0.3°$ and a random phase. Surrounding annuli were oriented randomly in each trial −20° or +20°, with $\lambda = 0.3°$ and a random phase. The contrast of the stimuli was 100%. Observers were instructed to inspect the target, and to report its orientation as clockwise or counter-clockwise to vertical (no feedback). The target + surround stimuli were presented starting from 350 ms after the trial initiation ("TI no-jitter" experiment), or starting from 450 ms ± up to 100 ms ("onset jitter" experiment), for a duration of 200 ms.

2.4. Procedure

In all conditions, each daily session was preceded by a brief practice block with easy stimuli (this practice was repeated until close-to-perfect accuracy was achieved).

TAE experiments. Sessions consisted of blocks of 125 trials (lasting ~5 min), separated by 2-minute breaks of blank screen-free viewing. In the periphery experiments, observers ($N = 14$) performed 3–8 daily sessions, each with five blocks. In the fixation experiment, observers ($N = 12$) performed a single session with six blocks.

TI experiments. Sessions consisted of blocks of 190 trials (lasting ~5 min), separated by 2-minute breaks of blank screen-free viewing. Observers ($N = 10$ for the "TI no-jitter" experiment, and $N = 10$ for the "onset jitter" experiment) performed a single session with five blocks.

Note that the number of observers in the main experiment in this work (TAE in the periphery, $N = 14$) was relatively smaller than typically used to study individual differences. However, the number of repetitions per observer was relatively large (3–8 daily sessions of 625 trials, see Fig. B.1), permitting higher precision in the individual measurement. We did not observe large differences in TAE due to differences in the number of sessions. All experiments in this study, with the exception of the "TI no-jitter" experiment, were previously analyzed for the within-individual effects of RT (Dekel & Sagi, 2020b).

2.5. Analysis

2.5.1. Fitting the perceived orientation

The magnitude of TAE and TI was calculated based on the reported orientation (clockwise vs. counterclockwise) of the near-vertical targets (the Gabor patch for TAE, and the central sine-wave circle for TI). The perceived vertical orientation (PV) is the interpolated orientation having an equal probability for clockwise and counter-clockwise reports (50%) of the target. The PV was found separately for each context orientation (−20° and +20°). This was achieved by interpolation from a fit to a cumulative normal distribution (with lapse rates) of the psychometric function (the percent clockwise reports as a function of target orientation). Psignifit 3.0 software (Fründ, Haenel, & Wichmann, 2011) was used for fitting. Then, the TAE or TI magnitude was calculated as half the shift in PV between the two opposing adaptor or surround orientations (−20° vs. +20°), and, if relevant, averaged over the left and right target positions and over the different daily measurements.

We noted that an alternative measure of bias, $\text{Bias}_{\text{crit\_shift}}$, described in Appendix A (Eq. (A.1)), can be defined from signal detection theory (Green & Swets, 1966). We found this alternative measure to be more convenient for RT-based modeling (Dekel & Sagi, 2020b); however, we preferred using the shift in the psychometric function because (i) $\text{Bias}_{\text{crit\_shift}}$ is less convenient in practical use because of its saturation with a large bias, and, at least here, loss of most of the collected data (i.e., using a single target orientation to calculate bias discards the data of the other target orientations); (ii) the shift in the psychometric function is expected to be more robustly correlated with RT, because, based on the modeling, $\text{Bias}_{\text{crit\_shift}}$ is inversely proportional to the square-root of the time, whereas the shift in the psychometric function is inversely *linear* with time; (iii) last but not least, we preferred using a standard measure of TAE over a less standard one. Nevertheless, we verified that the main finding reported here, of a lower TAE in the slower observers, is found when measuring TAE using $\text{Bias}_{\text{crit\_shift}}$ (Eq. (A.1)) (data not shown).

To calculate JNDs (just noticeable differences), we used a multiple of the interpolated inverse slope of the psychometric function at the PV orientation. Specifically, we used the width of the interval over which the fitted cumulative Gaussian function rises from $\Phi(-0.5) = 0.31$ to $\Phi(+0.5) = 0.69$, corresponding to 1σ where σ is the fitted standard deviation (or, put differently, to a performance of 69% correct or $d' = 1$ between the pair of orientations at the edge of the found interval). This interval was corrected so that the upper and lower lapse rates (as measured by the fit) do not affect the JND. Where relevant, JNDs were calculated separately and then averaged over the −20° and +20° contexts, over the left and right target positions, and over the different daily measurements.

2.5.2. Reaction times (RTs)

As a measure of RT for an observer, we used the mean RT in trials having a vertical target orientation (RT_{vert}). The use of RT_{vert} is motivated by theory (see Eq. (A.11) in Appendix A, as well as Dekel and Sagi (2020b)). To show that our findings are theory independent (see section 3.5), we also considered RT_{pv}, the interpolated RT at the PV orientation of the mean RT vs. target orientation function (using cubic interpolation; interpolation done after averaging across daily measurements). In addition, we considered RT_{max}, the mean RT at the slowest target orientation. Where relevant, RT_{vert}, RT_{pv}, and RT_{max} were calculated separately and then averaged over the −20° and +20° contexts and over the left and right target positions. In addition, RT_{vert} and RT_{max} were averaged over the different daily measurements (with RT_{pv}, averaging across daily measurements was done prior to the interpolation).

2.5.3. Non-decision times (t_0)

The modeling in Appendix A predicts the dependence of bias and sensitivity on the duration of a decision process. In addition to this "decision time", the duration of RTs includes non-decision components, such as the time it takes to press the response key. Here, we assume that this "non-decision time", t_0, is fixed and independent of the decision time (see Discussion). In addition, based on the RT distributions (Ratcliff, 1978; Ratcliff et al., 2016), we estimated t_0 to be approximately 350 ms in all observers of all experiments. To justify this simplifying assumption, we used a software that fits the RT distributions to the drift diffusion model (DDM; Fast-DM software, Voss and Voss (2007)). Fitted values of the t_0 model parameter somewhat differed depending on fitting details (e.g., whether outliers are pruned, whether the inter-trial variability parameters are enabled, and whether the used trials were of a vertical target orientation or of a tilted target orientation). Generally, differences in t_0 were small, between observers (< 100 ms *SD*), and between experiments (~50 ms). Moreover, the decision time, $\text{RT}_{\text{vert}} - t_0$, was mostly independent of t_0. To accurately fit the RT distributions with DDM, more trials are required. Finally, we verified that using the differently fitted t_0 values of each observer and experiment leads to similar results as when using the fixed value of 350 ms.

2.6. Statistics

All statistical analyses were performed using MATLAB® R2019b

software.

To obtain a measure for the statistical significance of individual differences in a factor, we considered repeated measurements over different days, fitting a linear mixed-effects model with one overall intercept term and also one intercept term per observer, and reported the significance of an *F*-test of the null hypothesis that the coefficients of all observer terms are 0 (so only the overall intercept term remains). This analysis is only applicable for the periphery experiment, requiring multiple daily measurements. A similar linear model, fitting the individual identity as a random effect, was used to calculate the intra-class correlation coefficient (ICC), obtained as $\frac{\sigma_\alpha^2}{\sigma_\alpha^2+\sigma_\epsilon^2}$, where σ_α^2 is the variance of the fitted observer coefficients, and σ_ϵ^2 is the variance of the linear model prediction errors (Nakagawa & Schielzeth, 2010).

To obtain a measure for the co-variation of two factors, we used the Pearson correlation coefficient (R, or occasionally its square-root, R^2, which measures shared variation). The statistical significance was assessed using the standard approach of applying a two-tailed *t*-test after transforming the data using Fisher's *z*-transformation. An alternative approach of using a linear mixed-effects model showed the same results (with better significance), but it is only applicable for periphery data with multiple daily measurements.

To fit Eqs. (1) and (2) we used the "fitnlm" MATLAB function, which finds the least-squares fit. Fit quality was assessed by recording the proportion of explained variation by the fit (R^2), calculated by: $R^2 = \frac{\text{TSS}-\text{RSS}}{\text{TSS}}$ where TSS is the total sum of squares of the data and RSS is the residual sum of squares (i.e., prediction errors). Note that R^2 can be negative when the variance of the prediction errors is larger than the variance of the data.

3. Results

Using briefly presented Gabor patches (50 ms), we measured the shift in the estimated vertical orientation of a near-vertical Gabor ("target"), caused by previous exposure to a Gabor patch tilted -20° or $+20^\circ$ to vertical ("adaptor", 600 ms ISI) (Fig. 1B). This experiment was performed using Gabor patches presented at the near-periphery ($\pm 1.8^\circ$ eccentricity), permitting analysis based on the relative retinal positions of the adaptor and the target: the same position ("Retinotopic") or contra-lateral positions ("Non-retinotopic"). The results for both retinotopic and non-retinotopic measurements showed a shift in the perceived orientation in the direction that is *away* from the adaptor orientation, a phenomenon known as the tilt aftereffect (TAE).

The peripheral TAE measured large individual variability (see the y-axis of Fig. 2), showing, in the peripheral retinotopic measurement, magnitudes ranging from 0° to 2° (Mean ± *SD* of 1.04° ± 0.63°), and a low measurement error (within-individual *SEM* over daily repetitions of ~0.2°; daily repetition data at Fig. B.1). Statistically, the presence of an individual component in TAE was significant ($p = 1.9 \times 10^{-12}$, $F_{(13,57)} = 12.72$, ICC = 0.63, using linear mixed-effects models, see the Methods). The peripheral non-retinotopic measurement showed the same, albeit at weaker TAE magnitudes (Mean ± *SD* of 0.33° ± 0.36°, the individual component at $p = 1.6 \times 10^{-5}$, $F_{(13,57)} = 4.77$, ICC = 0.34).

3.1. Co-variation of RT and peripheral TAE

Importantly, reaction time (RT), measured for the vertical target orientation and hence denoted RT_{vert}, exhibited a dramatic individual variation, with values ranging from 500 to almost 2000 ms (see the x-axis of Fig. 2; Mean ± *SD* across observers of 920 ± 360 ms for the peripheral retinotopic measurement). This range seems especially large when taking into account the non-decision time, t_0, which, based on the RT distributions, we estimated to be about 350 ± 100 ms (Mean ± *SD* across observers, see the Methods). Considering the different daily repetitions (Fig. B.1), the presence of an individual component in RT_{vert} was statistically significant ($p = 6.0 \times 10^{-14}$, $F_{(13,57)} = 15.05$, ICC = 0.69, same for retinotopic and for non-retinotopic trials).

Remarkably, the variability in RT_{vert} was strongly and negatively correlated with the variability in peripheral TAE (Fig. 2), with the fast observers having much more TAE than the slow observers. Specifically, for the peripheral retinotopic measurement, we found TAEs of ~2° for observers with RTs of ~500 ms, and close to zero TAE for observers with RTs approaching 2000 ms (Fig. 2A) ($R^2 = 0.74$, $p = 8 \times 10^{-5}$, $t_{(12)} = -5.85$, two-tailed *t*-test following Fisher's *z*-transformation, see the Methods). The peripheral non-retinotopic measurement revealed the same trend, albeit for weaker TAEs (Fig. 2B) ($R^2 = 0.52$, $p = 0.004$, $t_{(12)} = -3.61$). Overall, variability in peripheral TAEs seems to be largely explained by RTs.

3.2. Individual variability and decision times

To explain the co-variation of RT and TAE, we considered the idea that decisions are made by an evidence-accumulation process with biased initial conditions, which leads to reduced TAE with decision time (see the Introduction and Appendix A) (Dekel & Sagi, 2020b). This is a general argument, and depending on modeling details, it can predict different rates of reduction in bias. Here, we considered the case where the rate of reduction in bias is inversely proportional to the decision time (i.e., RT minus non-decision time), as in Eqs. (A.10) and

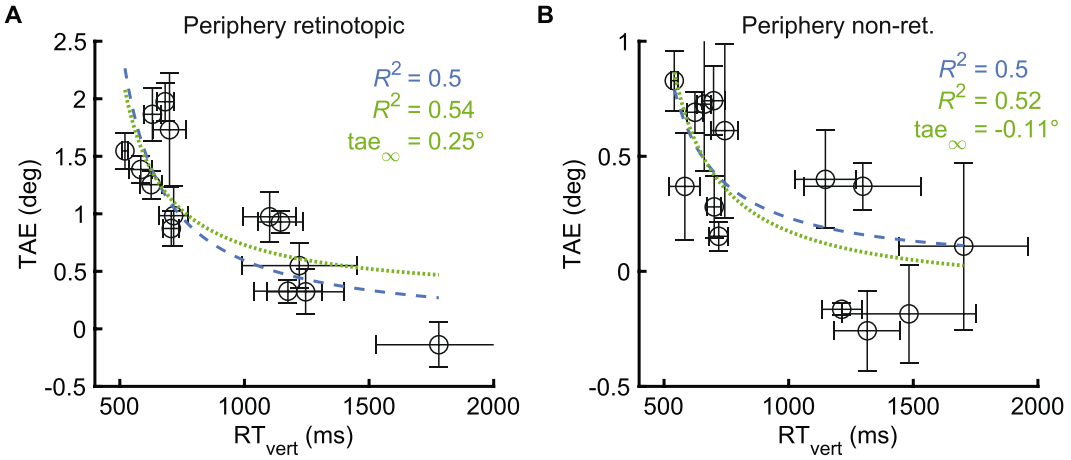

Fig. 2. Co-variation of RT and TAE: Shown is TAE as a function of the average RT for the vertical target, with each datum point corresponding to a different observer, in the (A) peripheral retinotopic and (B) peripheral non-retinotopic measurement. Blue dashed lines denote fits to Eq. (1), and green dotted lines denote fits to Eq. (2), when setting $t_0 = 350$ ms. Error bars are SEM across daily repetitions.

(A.16):

$$\mathrm{TAE} = \frac{\mathrm{tae}_0}{\mathrm{RT}_{\mathrm{vert}} - t_0} \quad (1)$$

where tae_0 is the bias constant, $\mathrm{RT}_{\mathrm{vert}}$ is the RT for a vertical target, and t_0 is the non-decision time (which reflects non-decision time components, such as the time it takes to press a response key, Ratcliff and McKoon (2008)). This equation reflects somewhat general assumptions that are broader than those of a single model. For example, Eq. (1) is predicted from an unbounded decision process (see Eq. (A.10)), and also from a bounded decision process with variability in the size of the separation between the bounds (see Eq. (A.16)). Note that Eq. (1) assumes that the intrinsic orientation sensitivity (v_0 in Appendix A) is approximately fixed in the sampled population (see the relevant Results section below, in the Discussion, and see Eq. (A.17)).

We also considered the possibility of a time-independent bias component, tae_∞, that is additive with the time-dependent bias of Eq. (1):

$$\mathrm{TAE} = \frac{\mathrm{tae}_0}{\mathrm{RT}_{\mathrm{vert}} - t_0} + \mathrm{tae}_\infty \quad (2)$$

Time-independent bias can be mediated by a context-dependent change in the rate of evidence accumulation (drift rate bias, see section "time-independent bias" in Appendix A, and section "RT-independent bias" in the Discussion).

To account for individual differences using Eqs. (1) and (2) (resulting fits in Fig. 2), we assumed that tae_0, tae_∞ and the non-decision time (t_0) are approximately fixed in the population. Based on the RT distributions, we set $t_0 = 350$ ms (see section "Non-decision times (t_0)" in the Methods). Fitting tae_0 to behavior using Eq. (1) showed that 50% of the variability in peripheral TAEs can be explained by RT (retinotopic and non-retinotopic measurements showing $R^2 = 0.50$, Fig. 2). Note that the reduction in bias predicted by the fitted model is quite dramatic: from about 2° when RT = 500 ms, to about 0.5° when RT = 2000 ms in the peripheral retinotopic TAE (Fig. 2A). Fitting both tae_0 and tae_∞ using Eq. (2) showed similar R^2 values compared with the fit using Eq. (1) (peripheral retinotopic: $R^2 = 0.54$ with $\mathrm{tae}_\infty = 0.25° \pm 0.23°$; peripheral non-ret.: $R^2 = 0.52$ with $\mathrm{tae}_\infty = -0.11° \pm 0.14°$, Estimate ± *SE*).

3.3. Co-variation of RT and bias: The effects of experience

Next, we restricted the analysis of peripheral TAE to the first experimental session, to minimize potential interaction with perceptual learning (Yehezkel, Sagi, Sterkin, Belkin, & Polat, 2010). Results showed that the correlation between TAE and $\mathrm{RT}_{\mathrm{vert}}$ in the first session is maintained, even stronger, than when measurements are averaged across days (Fig. 3AC) (peripheral retinotopic: $R^2 = 0.68$, $p = 0.0005$, $t_{(11)} = -4.87$, peripheral non-ret.: $R^2 = 0.5$, $p = 0.007$, $t_{(11)} = -3.33$; one observer was not included in the analysis because of prior participation in a similar experiment). Similarly, fitting to Eq. (1) showed possibly better fits (peripheral retinotopic: $R^2 = 0.69$, peripheral non-ret.: $R^2 = 0.45$). This finding suggests that perceptual learning does not mediate the correlation of $\mathrm{RT}_{\mathrm{vert}}$ and TAE. The improved correlations compared to when measurements are averaged across days may reflect the larger variation in RTs (*SD* of ~550 ms compared with ~350 ms), or possibly that aggregating measurements across days having different RTs dilutes the observable effect of RT. Fits to Eq. (2) showed minor increase in R^2 compared with the fits to Eq. (1) (peripheral retinotopic: $R^2 = 0.71$ with $\mathrm{tae}_\infty = 0.2° \pm 0.21°$; peripheral non-ret.: $R^2 = 0.48$ with $\mathrm{tae}_\infty = -0.2° \pm 0.26°$, Estimate ± *SE*).

In the last session per observer (Fig. 3BD; day 5 ± 2, Mean ± *SD*), between-observer variation in $\mathrm{RT}_{\mathrm{vert}}$ was much reduced (*SD* of ~220 ms) compared with that on the first day, a typical effect of practice (Harris & Sagi, 2018; Sagi, 2011); however, the correlation with peripheral TAE was still significant for the retinotopic TAE case

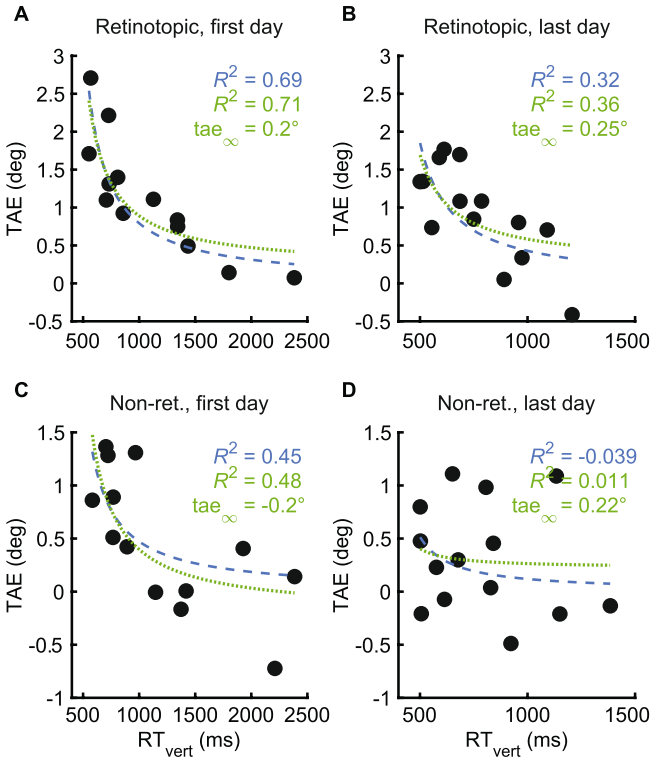

Fig. 3. Co-variation of RT and TAE: the effects of experience with the task. Same as Fig. 2, for the (A and C) first and (B and D) last experimental sessions, of the (A and B) retinotopic and (C and D) non-retinotopic measurement of the periphery experiment.

(peripheral retinotopic: $R^2 = 0.6$, $p = 0.001$, $t_{(12)} = -4.24$; peripheral non-ret.: $R^2 = 0.03$, $p = 0.5$, $t_{(12)} = -0.66$; exclusion of the same observer as above leads to the same results). Fits to Eq. (1) showed non-zero R^2 values only for the retinotopic case, and the differences between the fits to Eqs. (1) and (2) were small (see Fig. 3).

3.4. Co-variation of RT and bias at fixation (TAE and TI)

Next, we considered a TAE experiment, similar to the one above, in which both adaptors and targets were presented at fixation, hence measuring retinotopic adaptation. The results showed a similar negative correlation between $\mathrm{RT}_{\mathrm{vert}}$ and TAE; however, it was weaker than observed in the periphery (Fig. 4A) ($R^2 = 0.39$, $p = 0.03$, $t_{(10)} = -2.51$). We also considered two experiments that measured the tilt illusion (TI, Fig. 1A, the spatial analogue of the TAE). The results showed a negative correlation between $\mathrm{RT}_{\mathrm{vert}}$ and the TI, though again the correlation was somewhat weak (Fig. 4BC) (TI no-jitter: $R^2 = 0.49$, $p = 0.03$, $t_{(8)} = -2.79$; TI onset jitter: $R^2 = 0.47$, $p = 0.03$, $t_{(8)} = -2.66$).

Interestingly, the fits of behavior to Eq. (1) were quite poor (dashed blue lines in Fig. 4; Fixation TAE: $R^2 = 0.16$, TI no-jitter: $R^2 = 0.06$, TI onset jitter: $R^2 = -0.43$; the negative R^2 value indicates that the prediction errors had higher variance then the predicted behavioral data, see the Methods). Importantly, fitting to Eq. (2), which include an RT-independent bias term, tae_∞, showed better fits (dotted green lines in Fig. 4; Fixation TAE: $R^2 = 0.32$ with $\mathrm{tae}_\infty = 0.56° \pm 0.37°$; TI no-jitter: $R^2 = 0.41$ with $\mathrm{tae}_\infty = 1.2° \pm 0.55°$; TI onset jitter: $R^2 = 0.37$ with $\mathrm{tae}_\infty = 1.53° \pm 0.48°$, Estimate ± *SE*). It can be observed that the fitted RT-independent bias term was much larger than found for peripheral TAE ($\mathrm{tae}_\infty \approx 0$ in Figs. 2 and 3).

Overall, these findings replicate the observation made for peripheral TAE (Fig. 2), albeit with a weaker effect. The weaker effect can be possibly explained by (i) reduced variation in $\mathrm{RT}_{\mathrm{vert}}$ when tested at

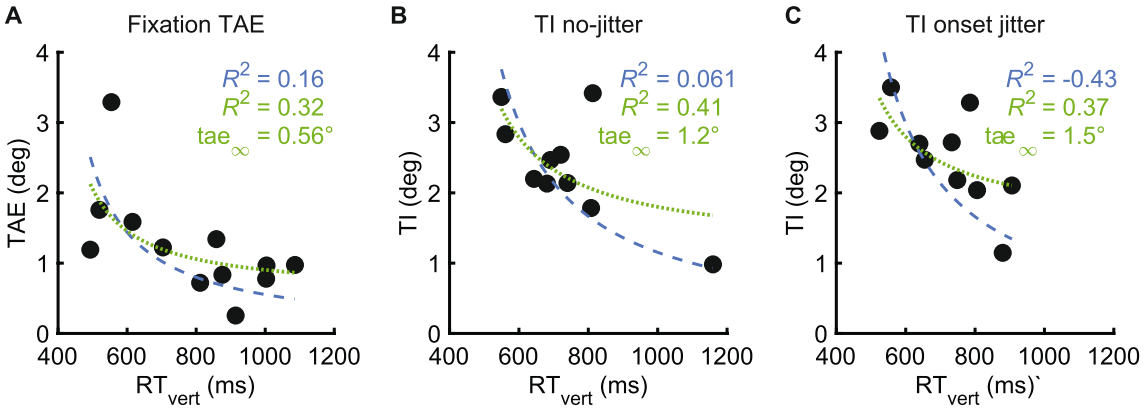

Fig. 4. Co-variation of RT and bias in fixation (TAE and TI). The same as Fig. 2, for (A) the fixation TAE experiment, (B) the TI experiment with a 200 ms presentation duration and no onset jigger, and (C) the TI experiment with a 200 ms presentation duration with an onset jigger. All experiments show a weak but significant correlation between bias magnitude and RT ($p < 0.05$).

fixation (compare x-axis of Figs. 2 and 4; "Fixation TAE": *SD* of 200 ms, "TI no-jitter": *SD* of 175 ms, "TI onset jitter": *SD* of 130 ms), (ii) less data per observer (3–8 daily sessions for TAE in the periphery, a single daily session for TAE in fixation and TI), or, most interestingly, (iii) the existence of a large RT-independent component in TAE and TI in these experiments, as indicated by the improved fits to Eq. (2) compared with Eq. (1) (see the Discussion).

3.5. Reaction times for non-vertical targets

So far, we considered the RTs of the hard-to-decide vertical targets (RT_{vert}). For increasingly tilted target orientations, the task of discriminating clockwise vs. counter-clockwise tilts is easier, and RTs were faster (consistent with the offered model, see Appendix A and Palmer, Huk, and Shadlen (2005)). For example, in peripheral retinotopic TAE, the easiest target orientations (± 12°) measured RTs in the range of 400 to 800 ms (showing Mean ± *SD* of 550 ± 110 ms), which is faster and less variable than found for the vertical targets (RT_{vert} showing 920 ± 360 ms; see x-axis of Fig. 2).

Importantly, under certain theoretical assumptions, context-dependent shifts in the psychometric functions can be accompanied by corresponding shifts in the chronometric functions (by chronometric function we refer to the target RT distribution as a function of target orientation). For example, the psychometric and chronometric biases are predicted to be identical if the TAE or TI are modeled as drift rate biases in the drift diffusion model (Dekel & Sagi, 2020b). To show that the correlations found here between TAE and RT are theory independent, we reproduced the correlation for the periphery experiment when using the RT at the perceived vertical orientation (RT_{pv}) (see Fig. B.4, compare with Fig. 2). Moreover, the found values of RT_{pv} and RT_{vert} were very similar (with peripheral retinotopic RT_{pv} - RT_{vert} showing −4 ± 73 ms, Fig. B.4C). Using RT_{max}, the RT at the slowest target orientation, showed the same (Fig. B.5). In addition, inspecting the chronometric functions (Fig. B.6) should impress upon the reader how small is the expected change in RT from a change in PV (if at all) compared with the range of individual differences in RTs. Overall, the large individual variation in RT_{vert} (see x-axis of Fig. 2) is not a consequence of a shift of the chronometric function.

3.6. Just noticeable differences (JNDs)

Using the orientation discrimination task, it is possible to obtain a measure for orientation sensitivity (i.e., JND, just noticeable differences, calculated as a multiple of the interpolated inverse slope of the psychometric function, see the Methods). Considering JNDs is interesting given previous work suggesting that individual variability in TI can be explained by individual variability in JNDs (Song et al., 2013) (see the Discussion). Here, results in the different daily repetitions of the periphery experiment (Fig. B.3) showed that individual differences in JND are statistically significant ($p = 3.2 \times 10^{-6}$, $F_{(13,57)} = 5.40$), with somewhat low test–retest reliability (ICC = 0.37) (in this analysis, the JNDs were averaged over the retinotopic and the non-retinotopic trials). Importantly, the results did not show any correlation between JND and TAE or TI (Fig. B.2) (periphery retinotopic: $R^2 = 0.01$, periphery non-ret.: $R^2 = 0.06$, fixation: $R^2 = 0.01$, TI no-jitter: $R^2 = 0.23$ with $p = 0.17$, TI onset jitter: $R^2 < 0.01$). Similarly, a negative correlation between JND and RT_{vert}, which is predicted by Appendix A, was rather low (Fig. B.3) (TAE fixation: $R^2 = 0.31$ with $p = 0.06$ for $t_{(10)} = 2.10$; TI no-jitter: $R^2 = 0.31$ with $p = 0.09$ for $t_{(8)} = -1.89$, all other conditions: $R^2 \leq 0.05$; correlations of 1/JND with RT_{vert} were very similar). The lack of correlations with JNDs may be explained by lack of variation in the sampled population, or to theoretical considerations (see the Discussion).

3.7. Are fast decisions caused by biased initial conditions?

As evident from changing b in Eq. (A.11), biased starting points inherently lead to faster decision times in the bounded decision model (DDM), even when the bound separation (a) is fixed. However, a fixed bound separation with a variable bias is unlikely to account for the correlation of bias and RTs observed here for the following reasons. (i) Fitting the peripheral retinotopic data to the DDM showed much better fits when b is fixed in the population, compared with when a is fixed in the population (log-likelihood of about −300 vs. −820; fits obtained using an exhaustive search over the a and b alternatives, and, for each alternative, finding the optimal drift rate and non-decision time using the fast-dm software, Voss & Voss, 2007). The same was found when using an unconstrained fit and correlating fitted a and b values with behavioral RT_{vert} (averaged within observer; correlation with a^2: $R^2 = 0.88$, $p = 7 \times 10^{-7}$, $t_{(12)} = 9.39$; correlation with b^2: $R^2 = 0.01$, $p = 0.72$, $t_{(12)} = 0.36$; again using fast-dm, but with a Kolmogorov-Smirnov setting and minimal outlier pruning). (ii) The peripheral retinotopic and non-retinotopic TAEs exhibited different magnitudes, but almost identical RTs (see x-axis of Fig. 2) (difference between retinotopic and non-retinotopic RTs showing Mean ± *SE* of −42 ± 93 ms), suggesting a negligible influence of bias on RT. (Indeed, this strong independence can be taken as evidence in favor of an unbounded over a bounded decision process, consistent with Dekel and Sagi (2020b)). (iii) Theoretically, as seen in Eq. (A.11), the b^2 term is subtracted from a large constant, so the range of possible RTs from changing b is more limited than from changing a.

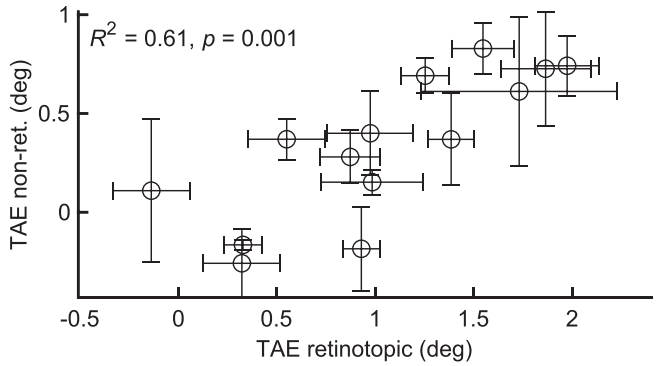

Fig. 5. Co-variation of retinotopic and non-retinotopic TAEs in the periphery experiment. Non-retinotopic TAE is shown as a function of retinotopic TAE, for different observers, averaged across daily repetitions. Error bars are SEM across repetitions.

3.8. Co-variation of peripheral retinotopic and non-retinotopic TAEs

In the periphery experiment, the retinotopic and non-retinotopic trials differed only in their relative target position, leading to very similar RTs in the two trial types ($R^2 = 0.94$ in the population; note that retinotopic and non-retinotopic trials were mixed within block balancing fatigue/motivation effects). Therefore, in the RT account of TAE described above, almost identical RTs were used in the retinotopic and the non-retinotopic cases (as evident in Fig. 2). Transitivity thus suggests a correlation between retinotopic and non-retinotopic TAEs, which was indeed found (Fig. 5) ($R^2 = 0.61, p = 0.001, t_{(12)} = 4.35$). A similar, though non-significant correlation was found between the TI and the fixation TAE effect magnitudes (five shared observers, $R^2 = 0.45, p = 0.21, t_{(3)} = 1.58$). This correlation is consistent with the idea of a common factor for similar visual phenomena (Grzeczkowski et al., 2017). Here, the common factor seems to be explained by RT, though a general account may also require other factors (such as JND, see the Discussion).

The strong correlation of non-retinotopic TAE with RT (Fig. 2) and with retinotopic TAE (Fig. 5) described above suggests that the non-retinotopic effect is not negligible, despite having a very small average magnitude ($M = 0.33^\circ$, $p = 0.005$, $t_{(13)} = 3.42$, two-tailed t-test; this measurement is approximately consistent with previous reports, Knapen et al., 2010).

3.9. Individual psychometric and chronometric functions

In the Methods and Appendix A, we make the standard assumption that $\Phi^{-1}(P_+)$ is approximately linear in the target orientation, where P_+ is the probability of clockwise answers, and Φ^{-1} is the inverse cumulative standard normal distribution function (see Macmillan and Creelman (2004)). The assumption was used for the modeling, and when fitting the psychometric function to a cumulative normal distribution for the purpose of measuring the TAE and the JND. To investigate if the assumption holds in the behavioral data, we consider the psychometric functions of the main condition (retinotopic TAE in the periphery). It can be observed that results (Fig. 6) indeed showed close to linear increase in $\Phi^{-1}(P_+)$ as a function of target orientation, for orientations around vertical, in practically all observers.

4. Discussion

4.1. RT-dependent bias

The results showed a large variability between individuals regarding their measured TAE magnitudes and moderate test–retest reliability. This variability is consistent with findings in earlier works for other context-dependent biases (Grzeczkowski et al., 2017; Song et al., 2013). The results also showed a large variation in RTs between individuals. In the periphery experiment, RTs ranged from ~500 ms to ~1800 ms when the target was vertical (Fig. 2). Importantly, the variability in TAE was strongly and negatively correlated with variability in RT (see Figs. 2–4). For example, in peripheral retinotopic TAE, the fastest observers had magnitudes of ~2°, whereas the slowest observers had almost no TAE. Note that here the time difference between the adaptation and test is always fixed; therefore, a slower RT does not correspond to increased adaptation decay (Greenlee & Magnussen, 1987; Magnussen & Johnsen, 1986). In the TI, we found similar albeit weaker correlations with RT (Fig. 4).

To explain correlations between perceptual bias and RT, we offer a quantitative theoretical framework based on known properties of human decision making (evidence accumulation theories, Gold & Shadlen, 2007; Ratcliff et al., 2016). The main idea considered in Appendix A is that bias reflects a change in the initial conditions, or priors, of an evidence accumulation decision process. In order to achieve a higher confidence level, decisions can be made slower, leading to individual differences in decision times. Importantly, we propose that the initial conditions are approximately fixed in the population. Thus, with increased decision time, the influence of the initial conditions is expected to be reduced, as measured by less bias in slower observers. To summarize, we explain the individual differences in bias by observers having different RTs (different confidence levels), but the same internal prior (see fits to Eq. (1) in Figs. 2–4; note the fixed b in modeling in Appendix A). This observation is important, both conceptually and technically, for understanding individual differences in vision. For example, when attempting to map the strength of measured aftereffects to internal visual priors (Pellicano & Burr, 2012; Tibber et al., 2013; Yang et al., 2013). Note that even when no evidence exists (e.g., a vertical target orientation), we still expect the influence of the prior to be reduced with decision time (see Appendix A). An alternative account, assuming a fixed decision bound with observer dependent bias, was much worse in explaining the current data (see the Results).

Behaviorally, we speculate that RT-dependent bias is consistent with mechanisms that calibrate visual perception. For example, a prior for the reference frame of an object that is gradually updated based on object details. With spatial context, as in the tilt illusion, “prior” is reasonable in terms of coarse-to-fine processing. Such priors can be determined by probabilistic inference using stimuli statistics, and remain largely invariant to neuronal constraints.

Recently, we used the same theoretical framework to explain RT-dependent bias within-individual, for the same experimental data (almost, see the Methods) (Dekel & Sagi, 2020b). The between- and within-individual effects are not necessarily a consequence of the same mechanism, so we were happy to find an explanation for both phenomena that is motivated by the same principles. Of course, the translation of theoretical concepts into psychological or physiological properties is somewhat speculative. We do not necessarily explain why some individuals are fast and others are slow, and the causal link between RT and perceptual bias remains speculative. Our hypothesis may be investigated in future work by manipulating the speed-accuracy tradeoff. It remains to be seen whether a fast and biased observer can become slow and unbiased given appropriate instructions. Note that in the periphery experiment, the number of daily repetitions differed between observers (see Fig. B.1). Importantly, the correlation of RT and TAE was observed in the first daily session when the observers were naïve (Fig. 3AC), and also in the last session when the observers were practiced (for the peripheral retinotopic TAE, Fig. 3B).

4.2. RT-independent bias

In evidence accumulation theories of the kind considered in this work, decision bias can be classified into two types: “start point bias” (bias reflecting a change in the initial conditions of evidence

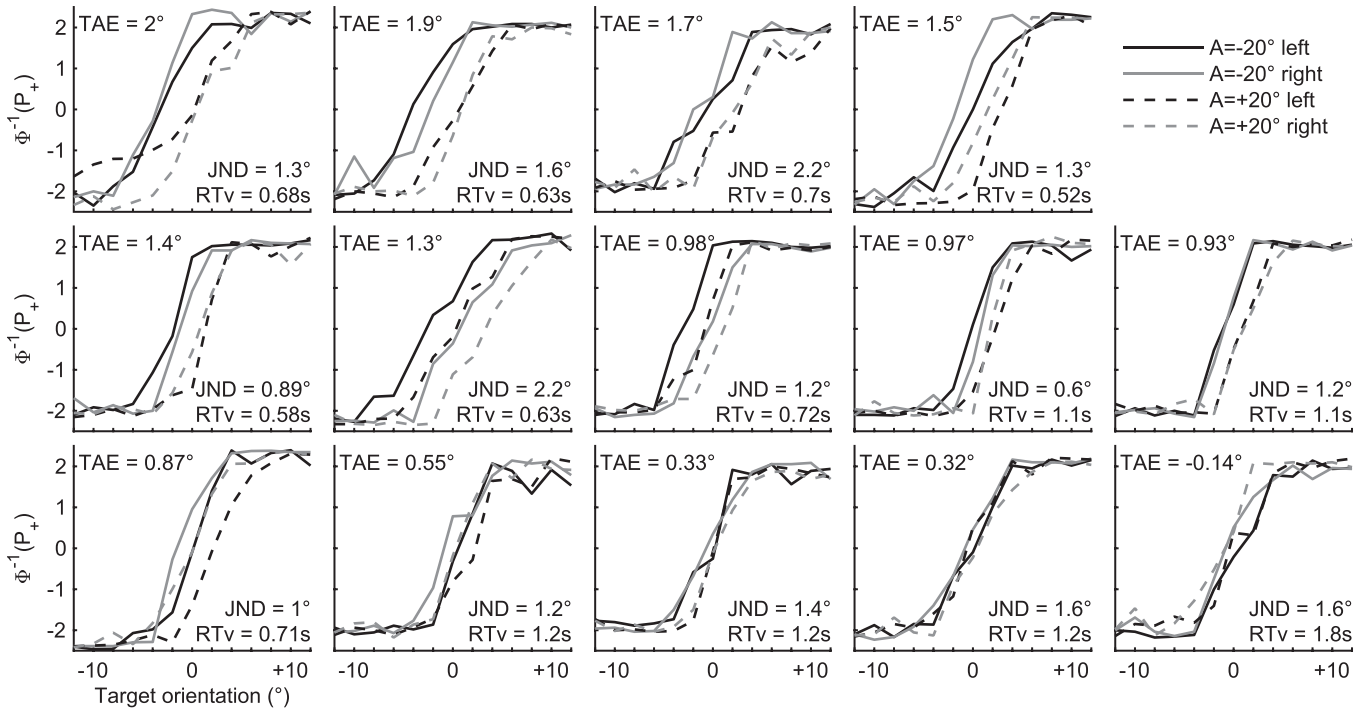

Fig. 6. Individual psychometric functions. Shown, for each observer in the retinotopic peripheral TAE measurement, are the four measured psychometric functions corresponding to two adaptor orientations ($-20°$ and $+20°$) and two sides of visual field (left and right of fixation, $\pm$ 1.8° eccentricity). Probabilities were clipped to the range $\left[\frac{1}{2n}, \frac{2n-1}{2n}\right]$, where n is the number of trials in a measurement. The written TAE and RT values were reproduced from Fig. 2A. It can be observed that around vertical (0°), the measured $\Phi^{-1}(P_+)$ is approximately linear in target orientation.

accumulation), and "drift rate bias" (bias reflecting a change in how evidence is accumulated) (Summerfield & De Lange, 2014). The former predicts time-dependent bias, as in Eq. (1). The latter usually predicts time-independent bias, unlike observed behaviorally. Importantly, behavioral biases such as TAE and TI may reflect a sum over different underlying mechanisms (Bao & Engel, 2012; Dekel & Sagi, 2020a). Possibly, not all bias mechanisms are RT-dependent. Consequently, Eq. (2) extends Eq. (1) with an additive RT-independent bias component reflecting a context-dependent change in the rate of evidence accumulation (see Appendix A). Fitting using Eq. (2) showed much improved fits than observed with Eq. (1) for the TI experiments (Fig. 4BC), possibly in agreement with the within-individual analysis considered in (Dekel & Sagi, 2020b).

4.3. Interpretations of fitted parameters

Eqs. (1) and (2) have three parameters: t_0, tae_0, and tae_∞. The t_0 is interpreted as the non-decision time, that is, all the non-decision factors such as stimulus encoding and motor movements (Ratcliff et al., 2016). Values of t_0 can also include decision components that are not included in DDM (Rüter, Sprekeler, Gerstner, & Herzog, 2013). Note that t_0 is obtained from the RT distributions (see the Methods), not by fitting of Eqs. (1) or (2). For simplicity, we used a fixed value of 350 ms for t_0 for all observers of all experiments (see the Methods). The tae_0, based on the Appendix A modeling, is a ratio between the starting point (b) and the intrinsic sensitivity (v_0) parameters (see Eqs. (A.8) and (A.14)). The starting point parameter, b, quantifies bias independently of differences in sensitivity and in RT, conceptually similar to how bias is quantified by values of the SDT criterion in a way that can be independent to differences in d' (Green & Swets, 1966). The intrinsic sensitivity parameter, v_0, maps this bias into the stimulus space (orientation). This intrinsic sensitivity parameter does not show RT dependence, and, combined with RT, determines the JND (Eqs. (A.9) and (A.13); see below). The tae_∞ parameter can be interpreted as the component(s) of the bias that are time-independent (discussed above, see Discussion on RT-independent bias).

4.4. Orientation sensitivity (JND)

Context-dependent biases can be positively correlated with measured orientation sensitivity (JND), both within-observer (Solomon & Morgan, 2006), and between observers (TI: Song et al., 2013, color and face aftereffects: Mattar, Carter, Zebrowitz, Thompson-Schill, & Aguirre, 2018). A JND-dependent bias can be predicted in evidence accumulation theories from individual differences in the rate (Eq. (A.17)) or the duration (Eqs. (A.10) and (A.16)) of the evidence. Similar to bias, the decision time is also predicted to be (negatively) correlated with JND (Eqs. (A.10) and (A.16)). However, here the results showed no correlation between JND and either TAE/TI or RT between observers (see the Results). We consider three ways to explain the lack of a strong correlations with JND in this work. First, by the smaller variation in JNDs in the sampled population here (approx. 0.5° to 2°) compared with previous work (approx. 0.5° to 6° in Song et al., 2013; note that their JND values are for 70.7% correct, while here JND values are for 69% correct, a negligible discrepancy). The smaller variation in JNDs found here may be attributed to measuring JNDs for perceived orientation (no physical reference), to rapid saturation of perceptual learning within the first session, or to the sampled population, which consisted of observers from the same age group (18–40) with comparable visual acuity (6/6). Second, by a discrepancy between the assumption using both models that the evidence is fixed in time, and the experiments, where the evidence was temporary (a target presentation duration of 50 ms for TAE and 200 ms for TI, with possibly a few hundred more milliseconds of persistence). This observation warrants caution when using simple models to interpret behavior. We emphasize that, for the purpose of this work, the analysis of RT and bias should be robust to a dynamic reduction in the evidence, because the found dependence of bias on RT persists in the case where there is no evidence

(i.e., $v = 0$; see Appendix A). Third, by reduced effect size when individual differences are measured using JND compared with RT or TAE. (That is, less between-observer variability compared to the within-observer measurement error.) Indeed, measured intra-class correlations (ICC) showed lower values for JND compared with retinotopic TAE and RT (0.37 compared with 0.63 and 0.69, respectively). Theoretically, reduced effect size for JND in the relevant measurement range is predicted from the Appendix A modeling (because JND squared is used in the proportionality equations, see Eqs. (A.10) and (A.16)). Generally, we expect a full account of individual variation in context-dependent bias to depend on both RT and JND.

4.5. Spatially non-selective TAE

Previous work suggested that the average TAE is very weak in non-retinotopic settings (i.e., when the adaptor and the target are presented at different retinal positions) (Knapen et al., 2010). We replicated this finding, but importantly, we found that the non-retinotopic TAE was strongly correlated with both RT (Fig. 2) and retinotopic TAE (Fig. 5). These findings suggest that the effect is more important than previously thought.

There is an ongoing attempt in the literature to classify measured biases as "perceptual" or "decisional" (e.g., Fritsche, Mostert, & de Lange, 2017; Morgan, 2014). While this classification is meaningful only within specific theoretical frameworks, we wish to make three general points. Firstly, that the kind of bias studied here – the TAE and the TI – is clearly at least partially perceptual (lends itself to visual experience), as evident by self-experimentation (try at Clifford, 2014; Thompson & Burr, 2009). This claim is supported by experiments (Morgan, 2014; Patten & Clifford, 2015). Secondly, that in the periphery experiment, we did not observe any qualitative difference between retinotopic and non-retinotopic TAEs, beyond a difference in magnitude. That is, both TAEs decayed to ~zero with increasing RTs, between and also within observers (Dekel & Sagi, 2020b). In addition, combinations of TAEs were well explained by additivity, regardless of retinotopicity (Dekel & Sagi, 2020a). Thirdly, that this work describes individual difference in measured TAE/TI explained as a consequence of a decisional factor (confidence), but, the starting point, that according to our analysis is stable across observers, we would like to believe is a sensory ("perceptual") factor.

CRediT authorship contribution statement

Ron Dekel: Conceptualization, Data curation, Formal analysis, Investigation, Methodology, Project administration, Software, Experiments, Statistics, Writing- Original draft preparation, Writing-Reviewing and Editing. **Dov Sagi:** Conceptualization, Funding acquisition, Investigation, Methodology, Supervision, Writing- Reviewing and Editing.

Acknowledgments

This research was supported by the Basic Research Foundation, administered by the Israel Academy of Science (Grant No. 6501560), and by The Weizmann Braginsky Center for the Interface between the Sciences and the Humanities. We thank Prof. Michael Herzog, an anonymous reviewer, Dr. Misha Katkov, Dr. Noga Pinchuk-Yacobi, and Michelangelo Naim for their helpful suggestions and comments.

Appendix A. Modeling using evidence accumulation

We consider two simple decision models that rely on accumulated evidence to make decisions, and try to estimate how model parameters relate to the behavioral measures of bias, sensitivity, and decision time. The models assume a temporal integration of evidence, at a fixed rate, with an initial state of accumulation that is set by prior evidence favoring (biasing) one decision outcome over others (Ratcliff, 1978; Ratcliff et al., 2016; Summerfield & De Lange, 2014) The integration of evidence is either stopped when a decision bound is reached (bounded model), or not (unbounded model), as detailed below. The modeling relies on signal detection theory (SDT, Green & Swets, 1966).

In the analysis, we make the following definitions: First, $\Phi^{-1}(\cdot)$ is the inverse cumulative standard normal distribution function. In addition, $\mathrm{Bias}_{\mathrm{crit\_shift}}$ is the bias (e.g., TAE) measured by the shift of an internal criterion between the contexts (Dekel & Sagi, 2020b; Green & Swets, 1966):

$$\mathrm{Bias}_{\mathrm{crit\_shift}}(c_1, c_2) = \Phi^{-1}(P_+^{c_1,\theta}) - \Phi^{-1}(P_+^{c_2,\theta}) \tag{A.1}$$

where $P_+^{c_1,\theta}$ is the probability of clockwise answers for target orientation θ under context c_1 (e.g., a vertical target and a -20° adaptor exposure), and $P_+^{c_2,\theta}$ is the same for context c_2 (e.g., the same target and a $+20^\circ$ adaptor exposure).

Finally, the orientation sensitivity between the orientations $+\theta$ and $-\theta$, namely $d'(\theta)$, can be defined as:

$$d'(\theta) = \Phi^{-1}(P_+^{c,+\theta}) - \Phi^{-1}(P_+^{c,-\theta}) \tag{A.2}$$

where $P_+^{c,+\theta}$ is the probability of clockwise answers for target orientation $+\theta$ under a given context c (e.g., a $+0.5^\circ$ target and a -20° adaptor exposure), and $P_+^{c,-\theta}$ is the same for target orientation -θ (e.g., a -0.5° target and the same adaptor).

We define JND (just noticeable difference) to be the inverse of $d'(\theta)$ evaluated at 2. Based on the experimental results (Fig. 6), we assume that $\Phi^{-1}(P_+^{c_1,\theta})$ is linear in target orientation θ (see Macmillan and Creelman (2004)). Thus, $d'(\theta)$ is linear in θ, with a proportionality constant that is the JND: $d'(\theta) = \frac{2\theta}{\mathrm{JND}}$. Rearranging, we get:

$$\mathrm{JND} = \frac{2\theta}{d'(\theta)} \tag{A.3}$$

Similarly, from the linearity of $\Phi^{-1}(P_+^{c_1,\theta})$ in θ, we get:

$$\mathrm{TAE} = \mathrm{Bias}_{\mathrm{crit\_shift}}(c_1, c_2) \cdot \frac{\theta}{d'(\theta)} \tag{A.4}$$

where TAE is bias measured in degrees (half the shift of the psychometric function between the contexts).

Unbounded model. Here, we consider a simple case without decision bounds (an unbounded model). Thus, we assume some process of evidence accumulation that is equivalent to a simple random walk (a Wiener process) that starts from point b (which is a scalar) and gradually diverges due to stochastic diffusion (noise) and drift v (the delta of evidence being accumulated at each time point). We expect the influence of the starting point of the random walk to diminish at a rate proportional to the square-root of the time. The probability density of the random walk at decision time t is a normal distribution with mean $b + v \cdot t$ and variance $\sigma^2 \cdot t$, namely, $\mathcal{N}(b + vt, \sigma^2 t)$, where σ^2 is the variance per unit time. Therefore,

$$\Phi^{-1}(P_+) = \frac{b + vt}{\sqrt{\sigma^2 t}} = \frac{b + vt}{\sigma\sqrt{t}} = \frac{b}{\sigma\sqrt{t}} + \frac{v}{\sigma}\sqrt{t} \tag{A.5}$$

where P_+ is the probability of the process being positive at time t.

The bias in the internal criterion ($\text{Bias}_{\text{crit\_shift}}$) is given by the change in $\Phi^{-1}(P_+)$ due to the context (see Eq. (A.1)), which is modeled as a change in the starting point ($+b$ compared with $-b$):

$$\text{Bias}_{\text{crit\_shift}}(c_1, c_2) = \Phi^{-1}(P_+^{c_1,\theta}) - \Phi^{-1}(P_+^{c_2,\theta}) = \frac{b + vt}{\sigma\sqrt{t}} - \frac{(-b) + vt}{\sigma\sqrt{t}} = \frac{2b}{\sigma\sqrt{t}} \tag{A.6}$$

And, similarly, the sensitivity (d'), given by the change in $\Phi^{-1}(P_+)$ due to a change in the stimulus ($+\theta$ compared with $-\theta$) (Eq. (A.2)), is modeled as a change in the drift rate ($+v$ compared with $-v$):

$$d'(\theta) = \Phi^{-1}(P_+^{c,+\theta}) - \Phi^{-1}(P_+^{c,-\theta}) = \frac{b + vt}{\sigma\sqrt{t}} - \frac{b + (-v)t}{\sigma\sqrt{t}} = \frac{2v}{\sigma}\sqrt{t} \tag{A.7}$$

Using Eqs. (A.3)–(A.7), we obtain:

$$\text{TAE} = \text{Bias}_{\text{crit\_shift}}(c_1, c_2)\cdot\frac{2\theta}{d'(\theta)} = \frac{2b}{\sigma\sqrt{t}}\cdot\frac{\theta}{\frac{2v}{\sigma}\sqrt{t}} = \frac{\theta b}{vt} = \frac{b}{v_0 t} \tag{A.8}$$

$$\text{JND} = \frac{2\theta}{d'(\theta)} = \frac{2\theta}{\frac{2v}{\sigma}\sqrt{t}} = \frac{\theta\sigma}{v\sqrt{t}} = \frac{\sigma}{v_0\sqrt{t}} \tag{A.9}$$

where v_0 is the intrinsic sensitivity, defined as $v_0 = \frac{v}{\theta}$. Note that v_0 is independent of θ, because, based on the assumptions above, $d'(\theta)$ is linear in θ, so the drift rate v of a target oriented θ is linear in θ.

We now consider how the different behavioral measures are predicted to change based on individual differences in the decision time t, when the intrinsic sensitivity (v_0) and the starting point (b) are assumed to be fixed in the population. Based on Eqs. (A.8) and (A.9), we get $\text{TAE} = O\left(\frac{b}{v_0 t}\right)$ and $\text{JND} = O\left(\frac{1}{v_0\sqrt{t}}\right)$, where $O(\cdot)$ is big-O notation for the variables b, v_0, and t. Therefore, when v_0 and b are fixed in the population, the following proportionality is predicted:

$$\text{TAE} \propto \text{JND}^2 \propto \frac{1}{t} \tag{A.10}$$

Note that the unbounded model does not explain the decision time itself, only how the decision time affects bias and sensitivity.

Bounded model (DDM). An alternative approach of modeling decision processes in the brain, which also explains decision times, is to assume that there are decision bounds. When the accumulated evidence reaches a bound, the process is stopped and a decision is made. Here we considered the standard bounded drift diffusion model (DDM, Gold & Shadlen, 2007; Ratcliff & McKoon, 2008; Ratcliff & Smith, 2015; Ratcliff et al., 2016; see mathematical background at Luce (1986), Shalden, Hanks, Churchland, Kiani, and Yang (2006)). The DDM can be defined using four parameters: the drift rate (v), bound separation (a), starting point (z), and non-decision time (t_0). In this description, the bounds are at 0 and a, and the process starts from the point z. We also define b as the distance of the starting point from the midpoint between the bounds: $b = z - \frac{a}{2}$.

Using Eq. (A.12) from (Palmer et al., 2005) for the case $v = 0$, we get: $\mathbf{E}[T_{\text{vert}}] = \frac{AB}{\sigma^2}$ where $\mathbf{E}[T_{\text{vert}}]$ is the expected decision time of vertical targets (for both upper and lower bounds), A and B are the distances from the starting point to the upper and lower bounds, respectively, and σ is the diffusion coefficient parameter that is usually set to a fixed value of 1 (Palmer et al., 2005). Therefore, using $A + B = a$ and $B = z = \frac{a}{2} + b$, and also assuming that $\frac{b}{a}$ is not too large so a^2 is much larger than b^2, we get:

$$\mathbf{E}[T_{\text{vert}}] = \frac{\left(\frac{a}{2} - b\right)\left(\frac{a}{2} + b\right)}{\sigma^2} = \frac{\left(\frac{a}{2}\right)^2 - b^2}{\sigma^2} \approx \frac{a^2}{4\sigma^2} \tag{A.11}$$

Moreover, using Eq. (A.6) from (Palmer et al., 2005) again for $v = 0$, we obtain $P_+ = \frac{B}{A+B} = \frac{1}{2} + \frac{b}{a}$, where P_+ is the probability to reach the upper bound. Because $\Phi^{-1}\left(\frac{1}{2} + x\right) \approx \sqrt{2\pi}x$ for small x values, we expect that when $\frac{b}{a}$ is not too large, it will approximately hold that $\Phi^{-1}(P_+) = \Phi^{-1}\left(\frac{1}{2} + \frac{b}{a}\right) \approx \sqrt{2\pi}\frac{b}{a}$. The bias, given by the change in $\Phi^{-1}(P_+)$ due to a change in context ($+b$ compared with $-b$, see Eq. (A.1)), for the case where $v = 0$, is given by:

$$\text{Bias}_{\text{crit\_shift}}(c_1, c_2) = \Phi^{-1}(P_+^{c_1,\theta}) - \Phi^{-1}(P_+^{c_2,\theta}) \approx \sqrt{2\pi}\frac{b}{a} - \sqrt{2\pi}\frac{(-b)}{a} \approx 5\cdot\frac{b}{a} \tag{A.12}$$

We consider now the task sensitivity. Using Eq. (A.13) from (Palmer et al., 2005) for the case of an unbiased starting point ($b = 0$), we obtain $P_+ = \frac{1}{1 + e^{-va/\sigma^2}}$. This is a logistic function, and thus, we can approximate it by $\Phi^{-1}(P_+) = \Phi^{-1}\left(\frac{1}{1 + e^{-\frac{va}{\sigma^2}}}\right) \approx \left(\frac{1}{2}\sqrt{\frac{\pi}{2}}\right)\cdot\frac{v\cdot a}{\sigma^2}$. As such, the sensitivity (d'), given by the change in $\Phi^{-1}(P_+)$ due to a change in stimulus (Eq. (A.2)), when $b = 0$, is given by:

$$d'(\theta) = \Phi^{-1}(P_+^{c,+\theta}) - \Phi^{-1}(P_+^{c,-\theta}) \approx \left(\frac{1}{2}\sqrt{\frac{\pi}{2}}\right)\left(\frac{v\cdot a}{\sigma^2} - \frac{(-v)\cdot a}{\sigma^2}\right) \approx \frac{5}{4}\cdot\frac{va}{\sigma^2} \tag{A.13}$$

Although Eq. (A.12) was derived when there is a small $\frac{b}{a}$ value and $v = 0$, and Eq. (A.13) was derived when $b = 0$, we found the approximations to be reasonably robust in the relevant parameter range (Fig. B.7).

Using Eqs. (A.3), (A.4), (A.12), and (A.13), the different behavioral measures can be approximated as following:

$$\mathrm{TAE} = \mathrm{Bias}_{\mathrm{crit\_shift}}(c_1, c_2)\cdot\frac{\theta}{d'(\theta)} \approx \frac{5b}{a}\cdot\frac{\theta}{\frac{5va}{4\sigma^2}} = \frac{4\theta b\sigma^2}{va^2} = \frac{4b\sigma^2}{v_0a^2} \tag{A.14}$$

$$\mathrm{JND} = \frac{2\theta}{d'(\theta)} \approx \frac{2\theta}{\frac{5}{4}\cdot\frac{va}{\sigma^2}} = \frac{4\theta\sigma^2}{5va} = \frac{4\sigma^2}{5v_0a} \tag{A.15}$$

where $v_0 = \frac{v}{\theta}$ is the intrinsic sensitivity (as above). Based on Eqs. (A.11), (A.14) and (A.15), we obtain $\mathbf{E}[T_{\mathrm{vert}}] \approx O(a^2)$, $\mathrm{TAE} \approx O\left(\frac{b}{v_0a^2}\right)$, and $\mathrm{JND} \approx O\left(\frac{1}{v_0a}\right)$, where $O(\cdot)$ is big-O notation for the variables b, v_0, and a. Therefore, from individual differences in the bound separation (a), and when assuming that the intrinsic sensitivity (v_0) and the starting point (b) are fixed in the population, the following proportionality is predicted:

$$\mathrm{TAE} \propto \mathrm{JND}^2 \propto \frac{1}{\mathbf{E}[T_{\mathrm{vert}}]} \tag{A.16}$$

where $\mathrm{E}[T_{\mathrm{vert}}]$ is the mean decision time for the vertical target.

In terms of the SPRT (Sequential Probability Ratio Test, Moran, 2015; Summerfield & De Lange, 2014; Wald, 1945), which is a standard Bayesian interpretation of the DDM, an increased bound separation corresponds to requiring lower type I and type II error rates, but starting from the same prior value (the b parameter). Hence, it seems reasonable to assume that the starting point remains the same when the bounds are changed. Specifically, in the DDM, when one of the decision alternatives is more likely than the other (having prior probabilities p and 1-p), it can be shown that the optimal placement of the starting point that minimizes the total error is given by $b = \frac{\log\left(\frac{p}{1-p}\right)}{4v}$ for $\sigma = 1$, which is independent of the bound separation (a). (The influence of the likelihood ratio $\frac{p}{1-p}$ on decision making has long been investigated using SDT, see e.g. Green and Swets (1966); we noted that an alternative modeling to the one offered here is to assume that the likelihood ratio $\frac{p}{1-p}$, rather than the starting point b, is fixed in the population.)

Time-independent bias. In all of the above modeling, we assumed that the TAE only results from a change in the starting point of the process (bounded or unbounded), leading to time-dependent bias. However, it is possible that the context leads to a change in both the starting point and the drift rate (see Dekel and Sagi (2020b)). In this sense, Eqs. (A.10) and (A.16) model the time-dependent component, with the total TAE having an additional time-independent, possibly additive, component. Indeed, if the change in drift rate is fixed across target orientations, then the time-independent component is equivalent to a shift of the psychometric function, and hence the time-dependent and time-independent components are additive. It is straightforward to edit Eqs. (A.10) and (A.16) to include an additive and time-independent TAE component.

Final remarks. As shown above, both models can predict the same dependence on decision time (Eqs. (A.10) and (A.16)). It is worthwhile to mention two important ways in which these models are over-simplified. First, both models assume zero noise at $t = 0$, which is clearly impossible in a biological system. Second, both models assume that the evidence is fixed in time; however, in many experiments (and here), the evidence is temporary (see the Discussion). Importantly, although modeling these constraints leads to a more complicated analysis, the TAE value is still expected to be reduced with decision time.

In addition, it seems interesting to extend the above analysis by considering individual differences in the intrinsic sensitivity (v_0) in addition to the decision time (t). For the unbounded model, based on Eqs. (A.8) and (A.9), we obtain $\mathrm{TAE} = O\left(\frac{b}{v_0t}\right)$ and $\mathrm{JND} = O\left(\frac{1}{v_0\sqrt{t}}\right)$, as above. Therefore, individual differences in both v_0 and t, assuming that the starting point (b) is fixed in the population, lead to the following proportionality:

$$\mathrm{TAE} \propto \frac{1}{\frac{1}{\mathrm{JND}\cdot\sqrt{t}}t} = \frac{\mathrm{JND}}{\sqrt{t}} \tag{A.17}$$

The same proportionality is found in the bounded model (DDM), for individual differences in the bound separation (a) and the intrinsic sensitivity (v_0), assuming a fixed starting point (b).

Appendix B. Supplementary data

Supplementary data to this article can be found online at https://doi.org/10.1016/j.visres.2020.08.002.

References

Andrews, D. P. (1964). Error-correcting perceptual mechanisms. *Quarterly Journal of Experimental Psychology, 16*(2), 104–115. https://doi.org/10.1080/17470216408416355.

Bao, M., & Engel, S. A. (2012). Distinct mechanism for long-term contrast adaptation. *Proceedings of the National Academy of Sciences, 109*(15), 5898–5903. https://doi.org/10.1073/pnas.1113503109.

Benucci, A., Saleem, A. B., & Carandini, M. (2013). Adaptation maintains population homeostasis in primary visual cortex. *Nature Neuroscience, 16*(6), 724–729. https://doi.org/10.1038/nn.3382.

Carandini, M., & Heeger, D. J. (2012). Normalization as a canonical neural computation. *Nature Reviews Neuroscience, 13*(1), 51–62.

Clifford, C. W. G. (2014). The tilt illusion: Phenomenology and functional implications. *Vision Research, 104*, 3–11. https://doi.org/10.1016/j.visres.2014.06.009.

Clifford, C. W. G., & Rhodes, G. (2005). *Fitting the mind to the world: Adaptation and after-effects in high-level vision, Vol. 2*. Oxford University Press.

Clifford, C. W. G., Webster, M. A., Stanley, G. B., Stocker, A. A., Kohn, A., Sharpee, T. O., & Schwartz, O. (2007). Visual adaptation: Neural, psychological and computational aspects. *Vision Research, 47*(25), 3125–3131. https://doi.org/10.1016/j.visres.2007.08.023.

Clifford, C. W. G., Wenderoth, P., & Spehar, B. (2000). A functional angle on some after-effects in cortical vision. *Proceedings of the Royal Society of London. Series B: Biological Sciences, 267*(1454), 1705–1710.

Coen-Cagli, R., Kohn, A., & Schwartz, O. (2015). Flexible gating of contextual influences in natural vision. *Nature Neuroscience, 18*(11), 1648–1655. https://doi.org/10.1038/nn.4128.

Day, R. H. (1972). Visual spatial illusions: A general explanation. *Science, 175*(4028), 1335–1340.

Dekel, R., & Sagi, D. (2020a). Interaction of contexts in context-dependent orientation estimation. Vision Research 169, 58–72. https://doi.org/10.1016/j.visres.2020.02.006.

Dekel, R., & Sagi, D. (2020b). Perceptual bias is reduced with longer reaction times during visual discrimination. Communications Biology 3(1), 1–12. https://doi.org/10.1038/s42003-020-0786-7.

Fritsche, M., Mostert, P., & de Lange, F. P. (2017). Opposite effects of recent history on perception and decision. *Current Biology*.

Fründ, I., Haenel, N. V., & Wichmann, F. A. (2011). Inference for psychometric functions in the presence of nonstationary behavior. *Journal of Vision, 11*(6).

Gibson, J. J. (1937). Adaptation, after-effect, and contrast in the perception of tilted lines. II. Simultaneous contrast and the areal restriction of the after-effect. *Journal of Experimental Psychology, 20*(6), 553–569. https://doi.org/10.1037/h0057585.

Gibson, J. J., & Radner, M. (1937). Adaptation, after-effect and contrast in the perception

of tilted lines. *Journal of Experimental Psychology, 20*(5), 453–467. https://doi.org/10.1037/h0059826.
Gold, J. I., & Shadlen, M. N. (2007). The neural basis of decision making. *Annual Review of Neuroscience, 30*, 535–574. https://doi.org/10.1146/annurev.neuro.29.051605.113038.
Green, D. M., & Swets, J. A. (1966). Signal detection theory and psychophysics.
Greenlee, M. W., & Magnussen, S. (1987). Saturation of the tilt aftereffect. *Vision Research, 27*(6), 1041–1043. https://doi.org/10.1016/0042-6989(87)90017-4.
Grzeczkowski, L., Clarke, A. M., Francis, G., Mast, F. W., & Herzog, M. H. (2017). About individual differences in vision. *Vision Research, 141*, 282–292. https://doi.org/10.1016/J.VISRES.2016.10.006.
Harris, H., & Sagi, D. (2018). Visual learning with reduced adaptation is eccentricity-specific. *Scientific Reports, 8*(1), 608.
Knapen, T., Rolfs, M., Wexler, M., & Cavanagh, P. (2010). The reference frame of the tilt aftereffect. *Journal of Vision, 10*(1), 1–13. https://doi.org/10.1167/10.1.8.
Kohn, A. (2007). Visual adaptation: Physiology, mechanisms, and functional benefits. *Journal of Neurophysiology, 97*(5), 3155–3164. https://doi.org/10.1152/jn.00086.2007.
Lamme, V. A. F., & Roelfsema, P. R. (2000). The distinct modes of vision offered by feedforward and recurrent processing. *Trends in Neurosciences, 23*(11), 571–579. https://doi.org/10.1016/S0166-2236(00)01657-X.
Luce, R. D. (1986). *Response times: Their role in inferring elementary mental organization.* Oxford University Press on Demand.
Macmillan, N. A., & Creelman, C. D. (2004). *Detection theory: A user's guide.* Psychology press.
Magnussen, S., & Johnsen, T. (1986). Temporal aspects of spatial adaptation. A study of the tilt aftereffect. *Vision Research, 26*(4), 661–672. https://doi.org/10.1016/0042-6989(86)90014-3.
Mattar, M. G., Carter, M. V., Zebrowitz, M. S., Thompson-Schill, S. L., & Aguirre, G. K. (2018). Individual differences in response precision correlate with adaptation bias. *Journal of Vision, 18*(13), 1–12. https://doi.org/10.1167/18.13.18.
Mollon, J. D., Bosten, J. M., Peterzell, D. H., & Webster, M. A. (2017). Individual differences in visual science: What can be learned and what is good experimental practice? *Vision Research, 141*, 4–15. https://doi.org/10.1016/j.visres.2017.11.001.
Moran, R. (2015). Optimal decision making in heterogeneous and biased environments. *Psychonomic Bulletin & Review, 22*(1), 38–53.
Morgan, M. J. (2014). A bias-free measure of retinotopic tilt adaptation. *Journal of Vision, 14*(1), 7.
Mulder, M. J., Wagenmakers, E. J., Ratcliff, R., Boekel, W., & Forstmann, B. U. (2012). Bias in the brain: A diffusion model analysis of prior probability and potential payoff. *Journal of Neuroscience, 32*(7), 2335–2343. https://doi.org/10.1523/JNEUROSCI.4156-11.2012.
Nakagawa, S., & Schielzeth, H. (2010). Repeatability for Gaussian and non-Gaussian data: A practical guide for biologists. *Biological Reviews, 85*(4), 935–956.
Palmer, J., Huk, A. C., & Shadlen, M. N. (2005). The effect of stimulus strength on the speed and accuracy of a perceptual decision. *Journal of Vision, 5*(5), 376–404. https://doi.org/10.1167/5.5.1.
Patten, M. L., & Clifford, C. W. G. (2015). A bias-free measure of the tilt illusion. *Journal of Vision, 15*(15), 8.
Pellicano, E., & Burr, D. (2012). When the world becomes "too real": A Bayesian explanation of autistic perception. *Trends in Cognitive Sciences, 16*(10), 504–510. https://doi.org/10.1016/j.tics.2012.08.009.
Pinchuk-Yacobi, N., & Sagi, D. (2019). Orientation-selective adaptation improves perceptual grouping. *Journal of Vision, 19*(9), 6. https://doi.org/10.1167/19.9.6.
Press, C., Kok, P., & Yon, D. (2020). The perceptual prediction paradox. *Trends in Cognitive Sciences, 24*(1), 13–24. https://doi.org/10.1016/J.TICS.2019.11.003.
Ratcliff, R. (1978). A theory of memory retrieval. *Psychological Review, 85*(2), 59.
Ratcliff, R., & McKoon, G. (2008). The diffusion decision model: Theory and data for two-choice decision tasks. *Neural Computation, 20*(4), 873–922. https://doi.org/10.1162/neco.2008.12-06-420.
Ratcliff, R., & Smith, P. (2015). Modeling simple decisions and applications using a diffusion model.
Ratcliff, R., Smith, P. L., Brown, S. D., & McKoon, G. (2016). Diffusion decision model: Current issues and history. *Trends in Cognitive Sciences, 20*(4), 260–281.
Rüter, J., Sprekeler, H., Gerstner, W., & Herzog, M. H. (2013). The silent period of evidence integration in fast decision making. *PloS One, 8*(1), https://doi.org/10.1371/journal.pone.0046525.
Sagi, D. (2011). Perceptual learning in Vision Research. *Vision Research, 51*(13), 1552–1566. https://doi.org/10.1016/J.VISRES.2010.10.019.
Salkind, N. (2012). Sequential tests of statistical hypotheses. *Encyclopedia of Research Design, 16*(2), 117–186. https://doi.org/10.4135/9781412961288.n414.
Schwartz, O., Hsu, A., & Dayan, P. (2007). Space and time in visual context. *Nature Reviews Neuroscience, 8*(7), 522–535. https://doi.org/10.1038/nrn2155.
Schwarzkopf, D. S., Song, C., & Rees, G. (2011). The surface area of human V1 predicts the subjective experience of object size. *Nature Neuroscience, 14*(1), 28–30. https://doi.org/10.1038/nn.2706.
Shadlen, M. N., Hanks, T. D., Churchland, A. K., Kiani, R., & Yang, T. (2013). The speed and accuracy of a simple perceptual decision: A mathematical primer. In Bayesian Brain (pp. 208–237). MIT Press Cambridge, MA. https://doi.org/10.7551/mitpress/9780262042383.003.0010.
Snow, M., Coen-Cagli, R., & Schwartz, O. (2017). Adaptation in the visual cortex: a case for probing neuronal populations with natural stimuli. F1000Research, 6.
Solomon, J. A., & Morgan, M. J. (2006). Stochastic re-calibration: Contextual effects on perceived tilt. *Proceedings of the Royal Society B: Biological Sciences, 273*(1601), 2681–2686.
Solomon, S. G., & Kohn, A. (2014). Moving sensory adaptation beyond suppressive effects in single neurons. *Current Biology: CB, 24*(20), R1012–22. https://doi.org/10.1016/j.cub.2014.09.001.
Song, C., Schwarzkopf, D. S., & Rees, G. (2013). Variability in visual cortex size reflects tradeoff between local orientation sensitivity and global orientation modulation. *Nature Communications, 4*, 2201.
Summerfield, C., & De Lange, F. P. (2014). Expectation in perceptual decision making: Neural and computational mechanisms. *Nature Reviews Neuroscience, 15*(11), 745.
Thompson, P., & Burr, D. (2009). Visual aftereffects. *Current Biology: CB, 19*(1), R11–4. https://doi.org/10.1016/j.cub.2008.10.014.
Tibber, M. S., Anderson, E. J., Bobin, T., Antonova, E., Seabright, A., Wright, B., ... Dakin, S. C. (2013). Visual surround suppression in schizophrenia. *Frontiers in Psychology, 4*, 88.
Voss, A., & Voss, J. (2007). Fast-dm: A free program for efficient diffusion model analysis. *Behavior Research Methods, 39*(4), 767–775.
Wald, A. (1945). Sequential tests of statistical hypotheses. *The annals of mathematical statistics, 16*(2), 117–186.
Webster, M. A. (2011). Adaptation and visual coding. *Journal of Vision, 11*(5).
Webster, M. A. (2015). Visual adaptation. *Annual Review of Vision Science, 1*, 547–567.
Wei, & Stocker. (2017). Lawful relation between perceptual bias and discriminability. Proceedings of the National Academy of Sciences 114(38), 10244–10249.
White, C. N., & Poldrack, R. A. (2014). Decomposing bias in different types of simple decisions. Journal of Experimental Psychology: Learning, Memory, and Cognition 40(2), 385.
Wolfe, J. M. (1984). Short test flashes produce large tilt aftereffects. *Vision Research, 24*(12), 1959–1964. https://doi.org/10.1016/0042-6989(84)90030-0.
Yang, E., Tadin, D., Glasser, D. M., Hong, S. W., Blake, R., & Park, S. (2013). Visual context processing in schizophrenia. *Clinical Psychological Science, 1*(1), 5–15.
Yehezkel, O., Sagi, D., Sterkin, A., Belkin, M., & Polat, U. (2010). Learning to adapt: Dynamics of readaptation to geometrical distortions. *Vision Research, 50*(16), 1550–1558.